Synthesis of Tetra-3-butenyl-Substituted Metallocenes and the Application of 1,1′,3,3′-Tetrakis(1,1-dimethyl-3-butenyl)ferrocene as Core for the Preparation of Polynuclear Compounds

Derk Vos, Alexander Salmon, Hans-Georg Stammler, Beate Neumann, and Peter Jutzi*

Fakultät für Chemie, Universität Bielefeld, 33615 Bielefeld, Germany

Received February 8, 2000

The synthesis of the 1,1′,3,3′-tetrabutenyl-substituted metallocenes $[C_5H_3(CMe_2CH_2CH{=}CH_2)_2]_2M$ (M = Fe **1**, Co **2**, Ni **3**), their electrochemical properties, and the solid-state structures of **1** and **3** are presented. Hydrosilylation of **1** with dimethylphenylsilane leads to $[C_5H_3(CMe_2(CH_2)_3SiMe_2Ph)_2]_2Fe$, **4**. The π-coordination ability of the arene system in **4** has allowed the preparation of the pentanuclear complex $[C_5H_3(CMe_2(CH_2)_3SiMe_2(\eta^6\text{-}C_6H_5{-}Cr(CO)_3)_2]_2Fe$, **5**, containing a ferrocene core and peripherial η^6-coordinated $Cr(CO)_3$ moieties. Electrochemical investigations of **5** show a reversible oxidation of the ferrocene unit as well as an independent, noninteracting irreversible oxidation of the Cr centers.

Introduction

The design and synthesis of polynuclear organometallic species has been a field of increasing interest in recent years. In particular, the combination of ferrocene units with the architectural diversity of dendrimer syntheses offers the possibility to generate new materials with interesting physical and chemical properties. In this context a number of dendrimers with redox-active peripheral as well as core units have been prepared.[1] Some of them already have resulted in applications such as multielectron reservoirs, amperometric biosensors,[2] or molecular recognition of small anions.[3] Furthermore, dendritic molecules with communicating peripheral ferrocenyl moieties have been prepared.[4]

We have focused our research on the synthesis and use of multifunctionizable metallocenes, which can act as starting cores for the synthesis of polynuclear organometallic complexes. In particular, ω-alkenyl-substituted metallocenes have been proven to be valuable precursors for the synthesis of redox-active macromolecules. The terminal double bonds allow a variety of functionalization reactions such as hydrosilylation, hydroboration, or the construction of highly branched dendritic molecules.[5]

Scheme 1

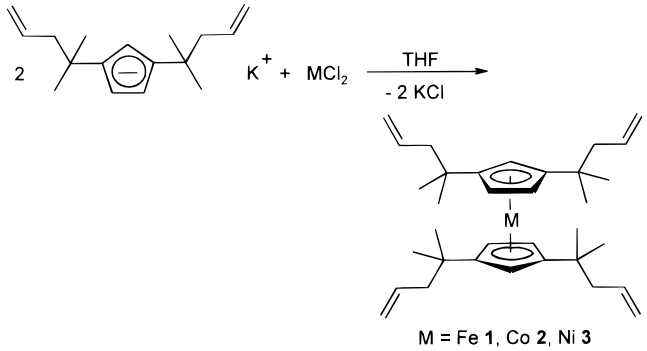

In this paper we report the synthesis and the electrochemistry of tetraalkenyl-substituted metallocenes of iron **1**, cobalt **2**, and nickel **3**. The use of ferrocene **1** as a starting core leads to the pentanuclear complex **5**, containing one Fe center and four peripheral Cr moieties. This system can be considered as the first generation dendrimer and might act as a model compound for higher generation dendrimers with interesting structural and electrochemical properties.

Results and Discussion

For the synthesis of the metallocenes **1**−**3**, potassium or lithium bis(1,1-dimethyl-3-butenyl)cyclopentadienides (Cp^BK/Li)[5b] were reacted with the corresponding metal dichlorides in THF (Scheme 1). Compounds **1**−**3** were isolated as viscous oils in good yield and characterized by means of IR spectroscopy, mass spectrometry, elemental analysis, and cyclic voltammetry. Furthermore, NMR studies have been performed with the diamagnetic ferrocene **1**.[6]

(1) For recent reviews see: (a) Newkome, G. R.; He, E.; Moorefield, C. N. *Chem. Rev.* **1999**, *99*, 1689−1746. (b) Hearshaw, M. A.; Moss, J. R. *J. Chem. Soc., Chem. Commun.* **1999**, 1−8. (c) Cuadrado, I.; Morán, M.; Casado, C. M.; Alonso, B.; Losada, J. *Coord. Chem. Rev.* **1999**, *193*, 3−195, 395−445. (d) *Dendritic Molecules*; Newkome, G. R., Moorefield, C. N., Vögtle, F., Eds.; VCH: Weinheim, 1996.

(2) Losado, J.; Cuadrado, I.; Morán, M.; Casado, C. M.; Alonso, B.; Barranco, M. *Anal. Chim. Acta* **1996**, *251*, 5.

(3) (a) Valerio, C.; Alonso, E.; Ruiz, J.; Blais, J.-C.; Astruc, D. *Angew. Chem.* **1999**, *111*, 1855. (b) Valerio, C.; Fillaut, J.-L.; Ruiz, J.; Guittard, J.; Blais, J.-C.; Astruc, D. *J. Am. Chem. Soc.* **1997**, *119*, 2588. (c) Casado, C. M.; Cuadrado, I.; Alonso, B.; Morán, M.; Losada, J. *J. Electroanal. Chem.* **1999**, *463*, 87.

(4) Cuadrado, I.; Casado, C. M.; Alonso, B.; Morán, M.; Losada, J.; Belsky, V. *J. Am. Chem. Soc.* **1997**, *119*, 7613.

(5) (a) Müller, C.; Vos, D.; Jutzi, P. *J. Organomet. Chem.* **2000**, *600*, 127. (b) Vos, D.; Jutzi, P. *Synthesis* **2000**, 357. (c) Batz, C.; Neumann, B.; Stammler, H.-G.; Jutzi, P. *Angew. Chem.* **1996**, *108*, 2272. (d) Batz, C.; Jutzi, P. *Synthesis* **1996**, 1296.

10.1021/om000118o CCC: $19.00
Publication on Web 08/18/2000

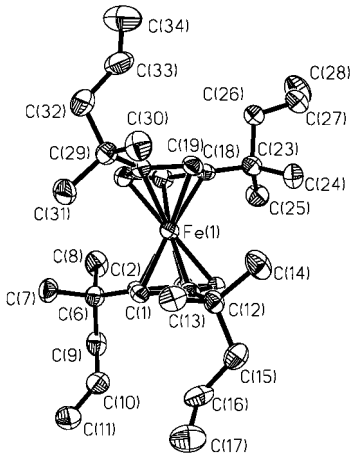

Figure 1. Molecular structure of $Cp^B{}_2Fe$, **1**, with thermal ellipsoids at 50% probability.

Crystals of **1** suitable for an X-ray structure analysis were obtained by cooling **1** without solvent to 4 °C. Compound **1** crystallizes in the triclinic space group $P\bar{1}$; its molecular structure is shown in Figure 1. Crystallographic data are provided in Table 1. Selected bond lengths and angles are collected in Table 2.

For the discussion of the solid-state structure, the following parameters are of main interest: (a) the torsion angle α of the Cp rings in the ferrocenyl skeleton relative to the ideal eclipsed conformation; (b) the tilt angle β of the Cp planes which indicates the deviation from a coplanar orientation of the Cp rings; (c) the bending angle γ which describes the variation of the C−C(Cp) vector from the plane of the corresponding Cp rings. Furthermore, the Cp(centroid)−Fe distances and the C−Fe bond lengths will be discussed. The two Cp rings of **1** are arranged in a conformation between eclipsed and staggered. The average torsion angle is α = 17.6° (triclinic Fc,[7] α = 9°; orthorhombic Fc,[8] α = 0°). Due to the high steric demand of the substitutents, the Cp rings are tilted about β = 7.9° from coplanarity. Furthermore, the side chains are bent away from the Fe center. The bending angles vary from 6.4° (C6) up to 10.4° for (C23). The high value for C23 is caused by the steric repulsion of the two alkyl substituents of the other Cp ligand (see Figure 2). The Cp(centroid)−Fe distances amount to 1.67 and 1.66 Å. The average Fe−C bond distance is 2.066(4) Å, which is slightly longer than in ferrocene (Fe−C: 2.052(2) Å) due to significant interannular interaction between the two Cp rings. Similar torsion (α = 15°; 18°) and tilt angles (β = 7°) are found in (t-$Bu_2C_5H_3)_2Fe$[9] or other ferrocenes with bulky substituents.[6b]

The paramagnetic cobaltocene **2** was isolated as a dark reddish-brown oil. The IR and MS data confirm the proposed structure of **2**. The nickelocene **3** was obtained as dark green crystals by cooling a toluene solution to 4 °C. The solid-state structure of **3** (Figure 3) is confirmed by X-ray crystal structure analysis. Crystallographic data are provided in Table 1. Selected bond lengths and angles are collected in Table 2.

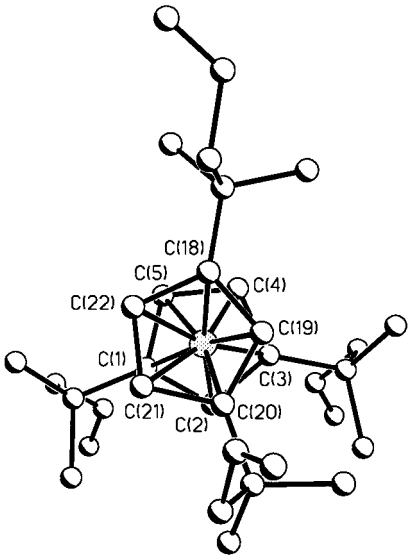

Figure 2. View along the Cp(centroid)−Fe vector.

The molecular structure of **3** is isomorphous with the structure of **1**. The average C(Cp)−Ni distance is 2.196(6) Å; this corresponds to a Cp(centroid)−Ni distance of 1.835 Å. The torsion angle is found to be α = 15.2°. The deviation of the Cp rings from parallel orientation is β = 7.2°. Again, the four substituents are bent away from the Ni center; the average bending is 6.2°. Compared to the molecular structure of **1**, these values indicate a lowered steric pressure of the bulky substitutents in **3**. The larger Cp(centroid)−M distance results in a smaller tilt angle. Furthermore, the side chains are bent away from the metal center to a lesser extent. The relative orientation of the Cp rings in **3** is closer to the ideal staggered conformation found in the parent compound Cp_2Ni.

The electrochemistry of the compounds **1**−**3** was studied by cyclic voltammetry (CV). The half-wave potentials are summarized in Table 3. As expected, the half-wave potentials are cathodically shifted compared to their parent compounds due to the inductive effect of the alkyl substituents. The oxidation of the ferrocene **1** and the cobaltocene **2** are both fully reversible. The CV of **3** is shown in Figure 4. Two oxidation steps from **3** to $\mathbf{3}^+$ and $\mathbf{3}^+$ to $\mathbf{3}^{2+}$ are detected. The peak separations for these processes indicate two reversible electron transfers. In contrast, the oxidation of Cp_2Ni to the dication is not electrochemically reversible.[10]

The alkenyl groups in the tetrafunctional ferrocene **1** enable further functionalization reactions. Hydrosilylation reactions are an excellent method to construct dendritic structures.[11] Hydrosilylation reaction of **1** with an excess of dimethylphenylsilane in the presence of Karstedt's catalyst (Scheme 2) gave ferrocene **4**, which was characterized by ^{1}H, ^{13}C, and ^{29}Si NMR and IR spectroscopy as well as by mass spectrometry.

Completion of the hydrosilylation reaction was evaluated in the ^{1}H NMR spectrum by the absence of the

(6) Variable-temperature NMR studies revealed a rotational barrier of ΔG = 14 kcal/mol. Similar rotational barriers have been found in ferrocenes with bulky substituents: (a) $(C_5H_3tBu_2)_2Fe$; ΔG =13.1 kcal/mol: Luke, W. D.; Streitwieser, A., Jr. *J. Am. Chem. Soc.* **1981**, *103*, 3241. (b) $(C_5H_3(SiMe_3)_2)_2Fe$; ΔG = 11 kcal/mol: Okuda, J.; Herdtweck, E. *J. Organomet. Chem.* **1989**, *373*, 99.

(7) Seiler, P.; Dunitz, J. D. *Acta Crystallogr.* **1979**, *B 35*, 2020.

(8) Seiler, P.; Dunitz, J. D. *Acta Crystallogr.* **1981**, *B 38*, 1741.

(9) Kaluski, Z. L.; Gusev, A. I.; Kalinin, A. E.; Struchkov, Y. T. *Zh. Strukt. Khim.* **1972**, *13*, 950.

(10) Kölle, U.; Khouzami, F. *Angew. Chem.* **1980**, *92*, 658.

(11) For examples see: (a) Zhou, L.-L.; Roovers, J. *Macromolecules* **1993**, *26*, 963. (b) Seyferth, D.; Son, D. Y.; Rheingold, A. L.; Ostrander, R. L. *Organometallics* **1994**, *13*, 2682.

Table 1. Crystallographic Data for Cp^B_2Fe, 1, and Cp^B_2Ni, 3

empirical formula	$C_{34}H_{50}Fe$ (**1**)	$C_{34}H_{50}Ni$ (**3**)
fw	514.59	517.45
cryst color, habit	yellow cuboid	green plates
cryst size, mm^3	0.10 × 0.20 × 0.40	0.70 × 0.50 × 0.10
temp, K	183(2)	173(2)
wavelength	Mo Kα 0.71073 Å (graphite monochromator)	
space group	triclinic, $P\bar{1}$	triclinic, $P\bar{1}$
unit cell dimens	a = 10.4298(8) Å	a = 10.460(6) Å
	b = 12.7176(10) Å	b = 12.941(9) Å
	c = 13.2150(10) Å	c = 13.041(10) Å
	α = 62.9510(10)°	α = 64.52(5)°
	β = 79.9950(10)°	β = 81.61(5)°
	γ = 73.2010(10)°	γ = 73.16(5)°
V, Å^3	1492.7(2)	1524.8(18)
Z	2	2
density (calcd), Mg/m^3	1.145	1.127
θ range for data collection, deg	1.73−27.18	1.73−22.5
no. of reflns collected	8757	4239
no. of ind reflns	6241 (R_{int} = 0.0304)	3974 (R_{int} = 0.0495)
abs corr	semiempirical from equivalents	
final R_F [$I>2\sigma(I)$]	0.0738 [4224]	0.0655 [2599]
wR_{F2} (all data)	0.1941	0.1703
no. of params	316	325
largest diff peak and hole, e Å^{-3}	1.631 and −0.618	0.486 and −0.815
diffractometer used	Siemens Smart CCD	Siemens P2(1)
programs used	Siemens SHELXTL plus/SHELXL-97	
structure refinement	full-matrix least-squares on F^2	
remarks	residual electron density 0.8 Å^{-3} from Fe1	

Table 2. Selected Bond Lengths (Å) and Angles (deg) for 1 and for 3

	(M = Fe) **1**	(M = Ni) **3**
M(1)−C(1)	2.053(4)	2.193(7)
M(1)−C(2)	2.065(4)	2.195(6)
M(1)−C(3)	2.098(4)	2.227(6)
M(1)−C(4)	2.055(4)	2.186(6)
M(1)−C(5)	2.044(4)	2.167(6)
Cp $(1)_{(centroid)}$−M(1)	1.671	1.834
M(1)−C(18)	2.063(4)	2.198(6)
M(1)−C(19)	2.065(4)	2.208(6)
M(1)−C(20)	2.100(4)	2.217(6)
M(1)−C(21)	2.063(4)	2.186(6)
M(1)−C(22)	2.055(4)	2.175(6)
Cp $(2)_{(centroid)}$−M(1)	1.677	1.835
torsion angle α	17.6	15.2
tilt angle β	7.9	7.2
Cp(1)−C(6)	6.4	6.3
Cp(1)−C(12)	7.6	6.0
Cp(2)−C(23)	7.1	4.6
Cp(2)−C(29)	10.4	7.8

Table 3. Half-Wave Potential of 1−3[a]

compound	$E_{1/2}$ [mV]
$Cp^B_2Fe/Cp^B_2Fe^+$	−220
$Cp^B_2Co/Cp^B_2Co^+$	−1410
$Cp^B_2Ni/Cp^B_2Ni^+$	−630
$Cp^B_2Ni^+/Cp^B_2Ni^{2+}$	490

[a] Scan rate: 100 mV/s. Referenced to internal Fc/Fc^+.

signals in the range from 4.50 to 7.00 ppm. Resonances due to the phenyl groups were found between 7.54 and 7.76 ppm. Additional signals due to methylene groups and the methyl groups attached to the silicon atom were present. ^{13}C and ^{29}Si NMR data confirm the proposed structure. In the ^{29}Si NMR spectrum, a resonance at −2.8 ppm was observed. Mass spectrometric analysis showed the molecular ion peak at m/z = 1058.

Ferrocene **4** is a suitable substrate for the synthesis of heterobimetallic complexes. The π-coordination ability of its peripheral arene rings offers a chance to connect

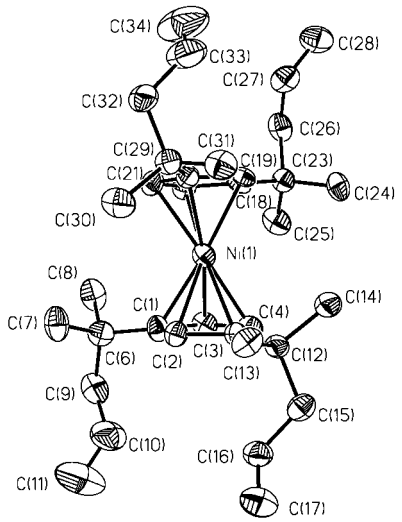

Figure 3. Molecular structure of Cp^B_2Ni, **3**, with thermal ellipsoids at 50% probability.

metal-containing fragments to the ferrocene core. Thermal treatment of **4** with an excess of $Cr(CO)_6$ in a 10:1 mixture of n-Bu_2O/THF led to the formation of **5**, which was isolated in moderate yield as a yellow oil (Scheme 2).

Several spectroscopic characteristics indicate the η^6-coordination of $Cr(CO)_3$ moieties. In the IR spectrum of **5**, two intense bands at 1975 and 1876 cm^{-1} are assigned to the carbonyl groups; in the ^{13}C NMR spectrum, the carbonyl group resonance is found at 233.0 ppm. The ^1H and ^{13}C NMR spectra provided additional information about the degree of phenyl complexation with $Cr(CO)_3$ fragments since the arene protons were shifted upfield ($\Delta\delta$ ∼2.5 ppm). This is due to a decreased ring current caused by a shielding of the $Cr(CO)_3$ groups.[12] In the ^1H NMR spectrum, only very weak signals in the range of 7.35−7.50 ppm could be

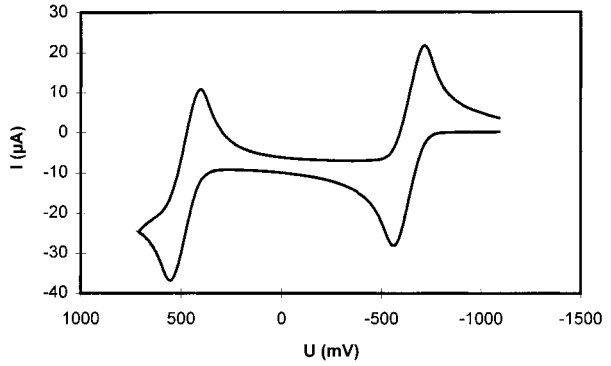

Figure 4. Cyclovoltammogram of **3**. Scan rate: 100 mV/s.

Scheme 2

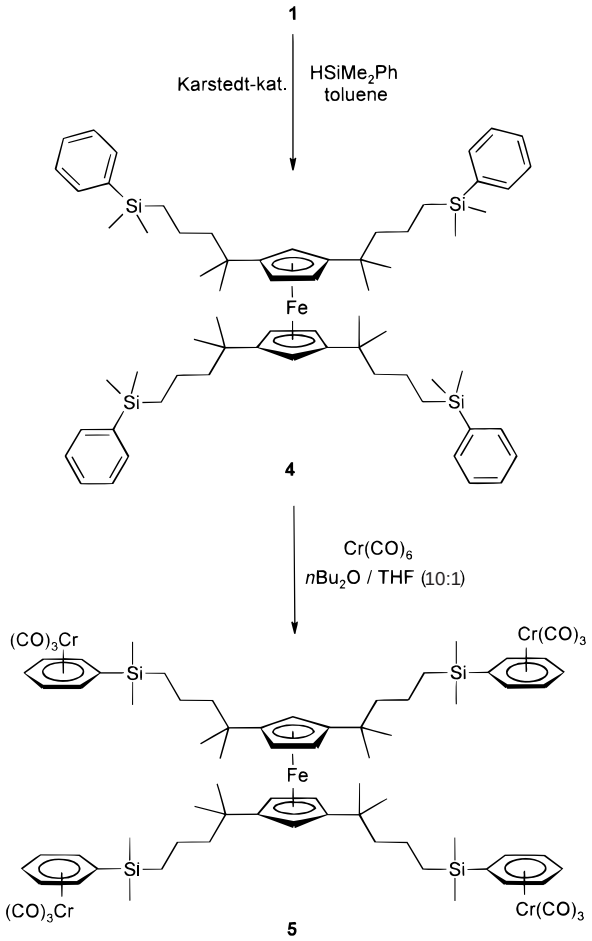

detected. These were assigned to noncomplexed arene ligands. On the basis of proton signal integration, less than 2% of the phenyl rings were not complexed with $Cr(CO)_3$ units. ^{13}C NMR data provided further evidence for an almost complete coordination of the arene rings. The ^{29}Si NMR showed only one resonance at 1.2 ppm. In the electrospray mass spectrum of **5**, the molecular ion peak was detected at $m/z = 1603$; the fragmentation was dominated by the loss of $Cr(CO)_3$ and $SiMe_2Ph$.

The electrochemistry of **5** has been studied using a nonnucleophilic solvent (CH_2Cl_2) and tetra-*n*-butylammonium hexafluorophosphate (TBAPF) as electrolyte. CV and the square wave voltammogram (SWV) show two independent oxidation peaks at −230 and 465 mV

(12) Price, J. T.; Sorensen, T. S. *Can. J. Chem.* **1968**, *46*, 515.

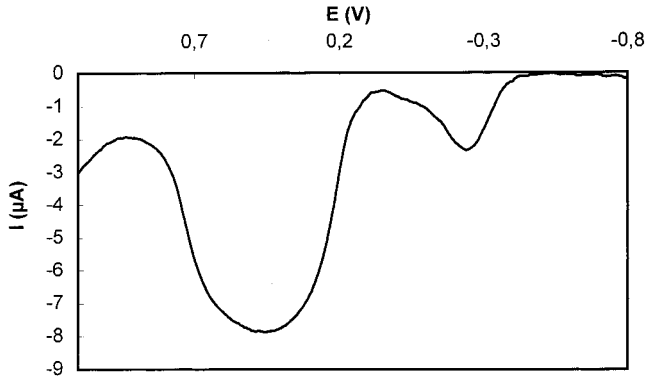

Figure 5. Square wave voltammogram of **5**. Scan rate: 50 mV/s.

(vs Fc/Fc^+), respectively. The square wave voltammogram of **5** is depicted in Figure 5. The first oxidation step at −230 mV was assigned to the ferrocene core. Oxidation of the Cr fragment was found to be irreversible, as could be evaluated from the half-width of the detected peaks ($\omega_{1/2} = 530$ mV) in the SWV and from the CV.[13] The results from cyclic and square wave voltammetry imply that the peripheral chromium tricarbonyl units do not interact electronically; thus they are oxidized independently. Analogous behavior of arene-chromium-tricarbonyl units has been observed in similar cases.[14] Even when two redox-active units are bound to one silicon center, no electronic communication between the neighboring groups was detected.

Experimental Section

General Procedure. Standard Schlenk techniques were used for the syntheses and sample manipulations. The solvents were dried by standard methods and distilled under argon prior to use. The reagents dimethylphenylsilane, $Cr(CO)_6$, and Florisil were procured commercially and used without further purification. Potassium/lithium 1,3-bis(1,1-dimethyl-3-butenyl)cyclopentadienide were prepared according to literature methods.[5b] Mass spectra (EI) were recorded on a Varian 311 A mass spectrometer (70 eV, 300 μA emission), ESI spectra on a Finnigan LCQ spectrometer. Only characteristic fragments and isotopes of the highest abundance are listed. NMR spectra were obtained using a Bruker Avance DRX 500 spectrometer (^1H, 500.1 MHz; ^{13}C, 125.75 MHz; ^{29}Si, 99.1 MHz); the spectra were referenced to the residual protons of the deuterated solvents. IR data were collected on a Bruker Vektor 22-FT-spectrometer. The samples were measured in solution between KBr windows or as KBr pellets. The melting point determinations were performed using a Büchi 500 melting point apparatus. Elemental analyses were performed by the Microanalytical Laboratory of the University of Bielefeld.

Electrochemical Measurements. Cyclic voltammograms and square wave voltammograms were recorded on a EG&G potentiostat model 273A, controlled by M 250/270 software. CH_2Cl_2 was freshly distilled from calcium hydride and deoxygenated by purging with purified argon. The supporting electrolyte was in all cases TBAPF, which was purchased from

(13) Electrochemical investigations of the parent compound $(C_6H_6)Cr(CO)_3$ under identical conditions revealed an irreversible oxidation, too.

(14) (a) Lobete, F.; Cuadrado, I.; Casado, C. M.; Alonso, B.; Morán, M.; Losada, J. *J. Organomet. Chem.* **1996**, *509*, 109. (b) Garcia, B.; Casado, C. M.; Cuadrado, I.; Alonso, B.; Morán, M.; Losada, J. *Organometallics* **1999**, *18*, 2349. (c) Rieke, R. D.; Tucker, I.; Milligan, S.; Wright, D. R.; Willeford, B. R.; Radonovich, L.; Eyring, M. *Organometallics* **1982**, *1*, 938.

Fluka and used without further purification. The supporting electrolyte concentration was 0.1 M. The voltammetric measurements were performed using a platinum disk electrode (d = 2 mm), which was polished prior to use. All potentials are referenced to the Fc/Fc^+ couple as internal standard. A platinum wire was used as a counter electrode. In general, the concentrations of the redox-active species were in the range 10^{-3} to 10^{-4} M.

$[C_5H_3(CMe_2CH_2CHCH_2)_2]_2M(II)$ (1−3). Potassium/lithium 1,3-bis(1,1-dimethyl-3-butenyl)cyclopentadienide dissolved in THF (20 mL) was added to a suspension of MCl_2 in THF (50 mL). The mixture was stirred at room temperature for 16 h. After removing all volatile products in vacuo, the residue was dissolved in toluene (50 mL) and filtered. The solvent was removed, and the respective metallocene was isolated as a viscous oil.

$[C_5H_3(CMe_2CH_2CHCH_2)_2]Fe$ (1). $LiCp^B$ (0.59 g, 2.5 mmol), $FeCl_2$ (0.16 g; 1.25 mmol). Compound **1** was isolated as an orange oil (0.59 g, 1.2 mmol, 92%). ^1H NMR ($CDCl_3$): δ 1.26 (s, 24H, CH_3), 2.11−2.16 (m, 8H, CH_2), 3.85 (s, 2H, CH_{ring}), 3.90 (s, 4H, CH_{ring}), 4.96 (d, 17.1 Hz, 4H, =CH_{trans}), 5.00 (d, 9.8 Hz, 4H, =CH_{cis}), 5.66 (s, br, 4H, =CH−). ^{13}C NMR ($CDCl_3$): δ 27.3 (CH_3), 34.0 (C_{quart}), 51.1 (CH_2), 64.8 (CH_{ring}), 97.4, 100.2 (C_{quart}), 116.8 (=CH_2), 136.1 (=CH−). IR (cm^{-1}): 1638 (C=C). MS (70 eV): m/z (%) 514 M^+ (100), 285 $M^+ - C_{17}H_{25}$ (75). Mp: 46 °C. Anal. Calcd for $C_{34}H_{50}Fe$ (M_r = 514.62): C, 79.35; H, 9.79. Found: C, 79.30; H, 10.40.

$[C_5H_3(CMe_2CH_2CHCH_2)_2]Co$ (2). $LiCp^B$ (1.18 g, 5.0 mmol), $CoCl_2$ (0.33 g; 2.5 mmol). Compound **2** was isolated as a dark brown oil (1.14 g, 2.2 mmol, 88%). IR (cm^{-1}): 3074, 2963, 1638 (C=C). MS (70 eV): m/z (%) 517 M^+ (100), 476 $M^+ - C_3H_5$ (2); 288 $M^+ - C_{17}H_{25}$ (52). Anal. Calcd for $C_{34}H_{50}Co$ (M_r = 517.71): C, 78.88; H, 9.73. Found: C, 78.74; H, 9.91.

$[C_5H_3(CMe_2CH_2CHCH_2)_2]Ni$ (3). KCp^B (1.34 g, 5.0 mmol), $NiCl_2$·DME (0.55 g; 2.5 mmol). Compound **3** was isolated as a green solid (1.21 g, 2.3 mmol, 92%). IR (cm^{-1}): 3074, 2963, 1639 (C=C). MS (70 eV): m/z (%) 516 M^+ (39), 287 $M^+ - C_{17}H_{25}$ (100); 204 $M^+ - NiC_{11}H_{14}$ (42), 41 $C_3H_5^+$ (7). Mp: 42−44 °C. Anal. Calcd for $C_{34}H_{50}Ni$ (M_r = 517.48): C, 78.92; H, 9.74. Found: C, 78.40; H, 9.73.

$[C_5H_3(CMe_2(CH_2)_3SiMe_2Ph)_2]_2Fe$ (4). Through a solution of **1** (0.20 g, 0.39 mmol) and Karstedts catalyst (0.5 mL, 1% in toluene) in toluene (50 mL) air was bubbled for 10 s. After stirring for 1 h at room temperature, dimethylphenylsilane (1.06 g, 7.8 mmol) was added. The reaction mixture was stirred for 10 h and then filtered through Florisil. The solvent and the excess dimethylphenylsilane were removed in vacuo. Compound **4** was isolated as a dark brown oil (0.40 g, 0.38 mmol, 97%). ^1H NMR ($CDCl_3$): δ 0.19 (s, 24H, SiCH_3), 0.58−0.61 (m, 8H, CH_2), 1.14−1.25 (m, 32H, CH_3, CH_2), 1.32−1.33 (m, 8H, CH_2), 3.69 (s, 2H, CH_{ring}), 3.80 (s, 4H, Cp-H), 7.31−7.36 (m, 12H, Ph-H), 7.44−7.46(m, 8H, Ph-H). ^{13}C NMR ($CDCl_3$): δ −2.8 (SiCH_3), 16.2, 18.8 (CH_2), 27.4 (CH_3), 33.3, 33.8 (C_{quart}), 50.2, 50.4 (CH_2), 63.3, 64.4, 64.8 (Fc-C), 97.2, 100.6 (C_{quart}), 127.6, 127.8, 127.9, 128.3, 128.7, 129.0, 132.9, 133.5, 134.1, 134.8, 135.2, 138.1, 139.7 (Ph-C). ^{29}Si NMR ($CDCl_3$): δ −2.8. MS (70 eV): m/z (%) 1058 M^+ (53); 922 $M^+ - Si(CH_3)_2$-PhH (19); 135 $Si(CH_3)_2Ph^+$. Anal. Calcd for $C_{66}H_{98}Si_4Fe$ (M_r = 1059.72): C, 74.81; H, 9.32. Found: C, 73.40; H, 9.28.[15]

$[C_5H_3(CMe_2(CH_2)_3SiMe_2(\eta^6\text{-}C_6H_5{-}Cr(CO)_3)_2]_2Fe$ (5). A solution of **4** (0.40 g, 0.38 mmol) and $Cr(CO)_6$ (0.83 g, 3.8 mmol) in 22 mL of THF/n-Bu_2O (ratio 1:10) was refluxed for 72 h. After cooling to room temperature, the reaction mixture was filtered through silica gel. All volatile products were removed in vacuo. The light orange residue was redissolved in hexane, and the solution was purified by column chromatography on silanized silica. Compound **5** was isolated as a yellow sticky oil (0.28 g, 1.7 mmol, 46%). ^1H NMR ($CDCl_3$): δ 0.17 (s, 24H, SiCH_3), 0.86 (s, br, 8H, CH_2), 1.35 (s, br, 24H, CH_3), 1.42 (s, br, 8H, CH_2), 1.52 (s, br, 8H, CH_2), 3.96 (s, br, 2H, Cp-H), 4.01 (s, br, 4H, Cp-H), 4.25−4.31 (m, 8H, Ph-H), 4.72−4.89 (m, 12H, Ph-H). ^{13}C NMR ($CDCl_3$): δ −3.0 (SiCH_3), 16.2, 19.2, 25.8 (CH_2), 27.7 (CH_3), 33.7, 34.2 (C_{quart}), 64.0, 64.8, 65.5 (Cp-C), 90.7, 92.4, 95.8, 99.4 (Ph-C), 97.8, 99.9 (C_{quart}), 233.7 (CO). ^{29}Si NMR ($CDCl_3$): δ 1.2 IR (cm^{-1}): 1975, 1876 (CO). MS (ESI, THF): m/z (%) 1603 $M^{\bullet+}$ (28); 1467 $M^+ - Cr(CO)_3$ (25); 1330 $M^+ - 2Cr(CO)_3$ (17). Anal. Calcd for $C_{78}H_{98}O_{12}Si_4Cr_4Fe$ (M_r = 1603.84): C, 58.41; H, 6.16. Found: C, 58.37; H, 6.77.

Acknowledgment. Financial support of the "Volkswagen-Stiftung" is gratefully acknowledged. D.V. thanks the "Fonds der Chemischen Industrie" for a fellowship. We thank Dr. H. Sievers for the measurement of the ESI-MS spectra.

Supporting Information Available: Tables of crystal data, positional and thermal parameters, and bond lengths and angles. This material is available free of charge via the Internet at http://pubs.acs.org.

OM000118O

(15) The discrepancies in the carbon value of the elemental analysis are most probably due to incomplete combustion of the material. Even the use of combustion catalysts do not lead to entirely satisfactory results.